

Research Article: Methods/New Tools | Novel Tools and Methods

neuTube 1.0: a New Design for Efficient Neuron Reconstruction Software Based on the SWC Format¹²³

neuTube: Efficient Neuron Reconstruction Software

Linqing Feng^{1,*}, Ting Zhao^{2,*} and Jinhyun Kim^{1,3}

¹Center for Functional Connectomics, Korea Institute of Science and Technology (KIST), Seoul, 136-791, Korea

²Janelia Research Campus, Howard Hughes Medical Institute, Ashburn, Virginia, 20147, United States

³Neuroscience Program, University of Science and Technology, Daejeon, 305-350, Korea

DOI: 10.1523/ENEURO.0049-14.2014

Received: 30 October 2014

Revised: 23 December 2014

Accepted: 23 December 2014

Published: 2 January 2015

Author Contributions: L.F., T.Z., and J.K. designed research; L.F. and T.Z. performed research; L.F. and T.Z. analyzed data; L.F., T.Z., and J.K. wrote the paper.

Funding: KIST Institutional Program
Project No. 2E24210

Funding: WCI Program
NRF Grant Number: WCI 2009-003

Funding: Howard Hughes Medical Institute

Conflict of Interest: Authors report no conflict of interest.

This work was supported by the KIST Institutional Program (Project No. 2E24210) and WCI Program (NRF Grant Number: WCI 2009-003). Ting Zhao is supported by Howard Hughes Medical Institute.

Correspondence should be addressed to: Dr. Ting Zhao, Janelia Research Campus, Howard Hughes Medical Institute, 19700 Helix Drive, Ashburn, VA 20147, United States (zhaot@janelia.hhmi.org), and Dr. Jinhyun Kim, Center for Functional Connectomics, Korea Institute of Science and Technology (KIST), 39-1 Hawolgokdong, Seoul, 136-791, Korea (kimj@kist.re.kr).

Cite as: eNeuro 2015; 10.1523/ENEURO.0049-14.2014

Alerts: Sign up at eNeuro.SfN.org to receive customized email alerts when the fully formatted version of this article is published.

Accepted manuscripts are peer-reviewed but have not been through the copyediting, formatting, or proofreading process.

This article is distributed under the terms of the Creative Commons Attribution License (<http://creativecommons.org/licenses/by/3.0>), which permits unrestricted use, distribution and reproduction in any medium provided that the original work is properly attributed.

Copyright © 2015 Society for Neuroscience

eNeuro

<http://eneuro.msubmit.net>

eN-TMNT-0049-14R1

neuTube 1.0: A New Design for Efficient Neuron Reconstruction Software
Based on the SWC Format

1
2
3
4
5
6
7
8
9
10
11
12
13
14
15
16
17
18
19
20
21
22
23
24
25
26
27
28

Manuscript Title Page

1. Manuscript Title (50 word maximum)

neuTube 1.0: A New Design for Efficient Neuron Reconstruction Software Based on the SWC Format

2. Abbreviated Title (50 character maximum)

neuTube: Efficient Neuron Reconstruction Software

3. List all Author Names and Affiliations in order as they would appear in the published article

Linqing Feng, Center for Functional Connectomics, Korea Institute of Science and Technology (KIST), Seoul, 136-791, Korea

Ting Zhao, Janelia Research Campus, Howard Hughes Medical Institute, Ashburn, Virginia, 20147, United States

Jinhyun Kim, Center for Functional Connectomics, Korea Institute of Science and Technology (KIST), Seoul, 136-791, Korea and Neuroscience program, University of Science and Technology, Daejeon, 305-350, Korea

4. Author Contributions: Each author must be identified with at least one of the following: Designed research, Performed research, Contributed unpublished reagents/ analytic tools, Analyzed data, Wrote the paper.

T.Z., L.F. and J.K. Designed Research; T.Z. and L.F. Performed Research; T.Z. and L.F. analyzed data; T.Z., L.F. and J.K. Wrote the paper.

L.F. and T.Z. contributed equally to this work.

5. Correspondence should be addressed to (include email address)

Dr. Ting Zhao, Janelia Research Campus, Howard Hughes Medical Institute, 19700 Helix Drive, Ashburn, VA 20147, United States (zhaot@janelia.hhmi.org) and Dr.

Jinhyun Kim, Center for Functional Connectomics, Korea Institute of Science and Technology (KIST), 39-1 Hawolgokdong, Seoul, 136-791, Korea (kimj@kist.re.kr)

6. Number of Figures: 6

29 **7. Number of Tables: 1**

30 **8. Number of Multimedia: 0**

31 **9. Number of words for Abstract: 170**

32 **10. Number of words for Significance Statement: 62**

33 **11. Number of words for Introduction: 412**

34 **12. Number of words for Discussion: 521**

35 **13. Acknowledgements**

36 The authors would like to thank Camden Markham for proof reading the manuscript
37 and thank Osung Kwon and Bokyoung Lee for testing the software.

38 **14. Conflict of Interest A. No (State 'Authors report no conflict**
39 **of interest') B. Yes (Please explain)**

40 A

41 **15. Funding sources**

42 This work was supported by the KIST Institutional Program (Project No. 2E24210)
43 and WCI Program (NRF Grant Number: WCI 2009-003). Ting Zhao is supported by
44 Howard Hughes Medical Institute.

45

46

47

48

49

50

51

52

53

54 **Abstract**

55 Brain circuit mapping requires digital reconstruction of neuronal morphologies in
56 complicated networks. Despite recent advances in automatic algorithms,
57 reconstruction of neuronal structures is still a bottleneck in circuit mapping due to a
58 lack of appropriate software for both efficient reconstruction and user-friendly
59 editing. Here we present a new software design based on the SWC format, a
60 standardized neuromorphometric format that has been widely used for analyzing
61 neuronal morphologies or sharing neuron reconstructions via online archives such
62 as NeuroMorpho.org. We have also implemented the design in our open-source
63 software called neuTube 1.0. As specified by the design, the software is equipped
64 with parallel 2D and 3D visualization and intuitive neuron tracing/editing functions,
65 allowing the user to efficiently reconstruct neurons from fluorescence image data
66 and edit standard neuron structure files produced by any other reconstruction
67 software. We show the advantages of neuTube 1.0 by comparing it to two other
68 software tools, namely Neuromantic and Neurostudio. The software is available for
69 free at <http://www.neutracing.com>, which also hosts complete software
70 documentation and video tutorials.

71 **Significance Statement**

72 Compared to other existing tools, the novel software we present has some unique
73 features such as comprehensive editing functions and the combination of seed-
74 based tracing and path searching algorithms, as well as their availability in parallel
75 2D and 3D visualization. These features allow the user to reconstruct neuronal

76 morphology efficiently in a comfortable ‘What You See Is What You Get’ (WYSIWYG)
77 way.

78 **1. Introduction**

79 Digital reconstruction, or tracing, of neuron morphologies from light microscope
80 images is an important step in the mapping of brain circuits. In this task, the input is
81 images and the output is usually a tree structure, which can be described by the
82 SWC file format (Cannon et al., 1998). Although numerous neuron reconstruction
83 software tools have been developed for producing SWC files (Meijering, 2010), none
84 of them has taken full advantage of the SWC format to optimize the user interface
85 for efficient and accurate reconstruction. An optimal user interface means that the
86 user can interact with the software with minimal cognitive load, which requires data
87 visualization to be clear and operations to be straightforward. In other words, with
88 the visual information provided by the software, the user should be able to quickly
89 figure out the underlying SWC model, how the model can be manipulated, and the
90 results of manipulations. With these criteria in mind, we may identify disadvantages
91 of many tracing software applications. For example, FARSIGHT (Luisi et al., 2011),
92 which focuses on semi-automated reconstruction of neurons, does not provide
93 intuitive low-level editing options to correct subtle errors. Simple Neurite Tracer, a
94 popular plugin of Fiji (Longair et al., 2011), also lacks editing functions. NeuroLucida,
95 a mainstream commercial software tool, allows complete manual reconstruction of
96 a neuron structure. However, it does not support neuron reconstruction in a 3D
97 visualization window, despite the fact that 3D interaction has been demonstrated to

98 improve both the speed and accuracy of the reconstruction procedure (Long et al.,
99 2012). Some other popular software tools, such as Neuromantic (Myatt et al., 2012)
100 and Neurostudio (Wearne et al., 2005), similarly lack advanced 3D editing functions.
101 On the other hand, Vaa3D (Peng et al., 2010) provides innovative interactive neuron
102 tracing functions in 3D, but these functions are not available in 2D to resolve dense
103 or faint structures.

104 Here, we propose a new and comprehensive software design based on the SWC
105 format as a solution to the diverse limitations of current tracing software. Based on
106 this design, or, as we call it, the SWC framework, we have converted our previously
107 reported software, neuTube (Kim et al., 2012), into a novel tool that enables efficient
108 reconstruction by combining robust automatic tracing algorithms and versatile
109 user-friendly editing functions in both 2D and 3D. This paper formally presents the
110 redesigned software, neuTube 1.0, not only as a major upgrade of the previous
111 release, but also as the first software to implement the SWC framework.

112 **2. Materials and Methods**

113 **2.1 The SWC framework**

114 The overall layout of the SWC framework is shown in Figure 1. Software with this
115 architecture takes a raw image or an SWC file as input and outputs a neuron
116 structure satisfying the user. The design of the SWC framework follows the principle
117 of ‘What You See Is What You Get’ (WYSIWYG) (Peng et al., 2011), *i.e.* what the user
118 is editing is explicitly visualized and no third-party viewer is needed to check the
119 results. Therefore, the SWC framework consists of the following features: clear
120 visualization of SWC structures, clear visualization of source images as reference

121 data, explicit definition of operation units and intuitive map from user inputs to
 122 editing operations. Except image visualization, these features are designed based on
 123 the SWC format, which describes a simple directed tree model, called the SWC
 124 model. Here, we described in detail how to construct operations on the SWC model
 125 by first defining the model in an abstract way.

126 **2.1.1 Abstract Definition of The SWC Model**

127 From a mathematical point of view, the SWC model can be defined as a set of nodes
 128 $\{\mathbf{n}_i = (x_i, y_i, z_i, r_i, \mathbf{n}_j) \mid i = 1, \dots, N, j = 0, \dots, N, i \neq j, x_i, y_i, z_i, r_i \in R\}$, where each
 129 node \mathbf{n}_i is a sphere with the center (x_i, y_i, z_i) and the radius r_i . \mathbf{n}_0 is an empty node
 130 for defining the roots of a neuron structure, and \mathbf{n}_j is called the parent of \mathbf{n}_i . An
 131 upstream path from \mathbf{n}_i to \mathbf{n}_j is an array of node $(\mathbf{n}_{k_1}, \dots, \mathbf{n}_{k_n})$ where $\mathbf{n}_{k_{i+1}}$ is the
 132 parent of \mathbf{n}_{k_i} , $k_1 = i, k_n = j$. To form a valid tree structure of a neuron, no loop is
 133 allowed, *i.e.* there is at most one upstream path from one node to another. In this
 134 model, the basic structural unit is a node, which defines how we should design
 135 visualization and interactions.

136 **2.1.2 SWC Operation**

137 Assuming S_1 and S_2 are two sets of nodes, the operation of a neuron structure is
 138 defined as

$$f(S_1) = S_2$$

139 For example, $f(\{\mathbf{n}_1, \dots, \mathbf{n}_n\}) = \phi$, where ϕ denotes the empty set, defines a removal
 140 operation. However, some operations may result in a new node set that forms an
 141 invalid neuron structure. How to construct a valid operation depends on the data
 142 structure describing the model. In our framework we used a redundant tuple to
 143

144 store a node, which is $\mathbf{n} = (G(\mathbf{n}), P(\mathbf{n}), C(\mathbf{n}), S(\mathbf{n}))$, where
 145 $G(\mathbf{n}) = (x(\mathbf{n}), y(\mathbf{n}), z(\mathbf{n}), r(\mathbf{n}))$ defines that the node is located at $(x(\mathbf{n}), y(\mathbf{n}), z(\mathbf{n}))$
 146 with radius $r(\mathbf{n})$, $P(\mathbf{n})$ is the *parent* node of \mathbf{n} , $C(\mathbf{n})$ is the first *child* of \mathbf{n} and $S(\mathbf{n})$ is
 147 the next *sibling* of \mathbf{n} . A sibling of \mathbf{n} shares the same parent with \mathbf{n} , i.e. $P(\mathbf{n}) =$
 148 $P(S(\mathbf{n}))$. The redundancy is designed to improve computational efficiency of visiting
 149 a node. For example, to query a child of a node, the program needs only to check its
 150 first child and traverse other children through the sibling link, while in a non-
 151 redundant representation where each node is only linked to its parent, the program
 152 may need to check every node in the tree.

153
 154 Editing a node \mathbf{n} is defined as changing the value of the corresponding tuple. We call
 155 any change on $G(\mathbf{n})$ a *geometrical operation* and any change on $P(\mathbf{n}), C(\mathbf{n})$ or $S(\mathbf{n})$ a
 156 *structural operation*. While a geometrical operation is straightforward, a structural
 157 operation may cause invalid neuron structures. For example, changing $P(\mathbf{n})$ alone
 158 may break the rule that $P(C(\mathbf{n})) = \mathbf{n}$ and $P(\mathbf{n}) = P(S(\mathbf{n}))$. To avoid this problem,
 159 we construct SWC operations at three levels in terms of operation complexity. The
 160 first level consists of three elementary operations linking a node \mathbf{n} to another node
 161 \mathbf{n}' , as defined as follows

$$162 \quad f_p(\{\mathbf{n}\}|\mathbf{n}') = f_p(\{(G(\mathbf{n}), P(\mathbf{n}), C(\mathbf{n}), S(\mathbf{n}))\}|\mathbf{n}') = \{(G(\mathbf{n}), \mathbf{n}', C(\mathbf{n}), S(\mathbf{n}))\}$$

$$163 \quad f_c(\{\mathbf{n}\}|\mathbf{n}') = f_c(\{(G(\mathbf{n}), P(\mathbf{n}), C(\mathbf{n}), S(\mathbf{n}))\}|\mathbf{n}') = \{(G(\mathbf{n}), P(\mathbf{n}), \mathbf{n}', S(\mathbf{n}))\}$$

$$164 \quad f_s(\{\mathbf{n}\}|\mathbf{n}') = f_s(\{(G(\mathbf{n}), P(\mathbf{n}), C(\mathbf{n}), S(\mathbf{n}))\}|\mathbf{n}') = \{(G(\mathbf{n}), P(\mathbf{n}), C(\mathbf{n}), \mathbf{n}')\}$$

165
 166
 167
 168

At this level, structure validity is not guaranteed.

169 The second level consists of simple valid operations. Assuming $F_{p_0}(\mathbf{n})$ is the
 170 operation of setting the parent of \mathbf{n} to \mathbf{n}_0 (the empty node), if $C(P(\mathbf{n})) = \mathbf{n}$, i.e. \mathbf{n} is
 171 the first child of its parent, then

172

$$F_{p_0}(\mathbf{n}) = \begin{cases} f_s(\{\mathbf{n}\}|\mathbf{n}_0) \circ f_p(\{\mathbf{n}\}|\mathbf{n}_0) \circ f_c(\{P(\mathbf{n})\}|S(\mathbf{n})), & C(P(\mathbf{n})) = \mathbf{n} \\ f_s(\{\mathbf{n}\}|\mathbf{n}_0) \circ f_p(\{\mathbf{n}\}|\mathbf{n}_0) \circ f_s(\{S^{-1}(\mathbf{n})\}|S(\mathbf{n})), & \text{Otherwise} \end{cases}$$

173

174 where $f \circ g$ denotes a composite operation and $S(S^{-1}(\mathbf{n})) = \mathbf{n}$. To define an
 175 operation on a single node more explicitly, $F_{p_0}(\mathbf{n})$ is defined as a function of a node
 176 instead of a node set without adding any ambiguity.

177

178 The operation of setting a parent is

179

$$F_p(\mathbf{n}|\mathbf{n}') = f_c(\{C(\mathbf{n}')\}|\mathbf{n}) \circ f_s(\{\mathbf{n}\}|C(\mathbf{n}')) \circ f_p(\{\mathbf{n}\}|\mathbf{n}') \circ F_{p_0}(\mathbf{n})$$

180

181 This operation also sets \mathbf{n} as the first child of \mathbf{n}' . In principle, this operation is
 182 sufficient for building all other operations. But in practice, it is useful to define one
 183 more operation, for setting a sibling:

184

$$F_s(\mathbf{n}|\mathbf{n}') = f_s(\{\mathbf{n}\}|\mathbf{n}') \circ f_s(\{\mathbf{n}'\}|S(\mathbf{n})) \circ f_p(\{\mathbf{n}'\}|P(\mathbf{n})) \circ F_{p_0}(\mathbf{n}')$$

185

186 The third level is a set of composition operations, which include any operation
 187 composed of the operations from the second level. At this level, we categorize the
 188 operations into two types, morphology-dependent and morphology-independent.
 189 An operation is morphology-dependent if the result of the operation depends on the
 190 positions or sizes of the nodes; otherwise it is morphology-independent.

191 Decomposing an operation into elementary operations helps guarantee the validity
 192 of neuron structure manipulation, and more importantly, helps implement the
 193 undo/redo functionality on arbitrary operations. An undo operation requires

194 inverting the corresponding operator, which can be complicated because of the
195 consistency requirement. For example, the inverse operation of deleting multiple
196 nodes would require recovery of all the neighbors of the nodes. Direct inference of
197 such an inverse operation not only takes significant effort, but also leads to errors
198 that can be difficult to track. After decomposing an operation into a sequence of
199 elementary operations, we can construct the undo operation easily by reversing the
200 sequence.

201

202 **2.1.3 User Interaction**

203 The fundamental function of tracing software is changing neuron morphology with
204 user inputs, which are usually composed of mouse clicks and key inputs. Since we
205 defined an operation as the mapping of one set of nodes to another set, user
206 interaction starts with node selection, which requires two components, SWC
207 visualization and user input response. High-quality visualization of a neuron might
208 be the most important feature of successful neuron editing. The ability to view the
209 structures clearly greatly reduces examination time needed to identify errors. It is
210 also necessary to provide both 2D and 3D views because each provides unique
211 advantages. For example, a 3D view is well suited for displaying a global structure;
212 and a 2D view provides precise inference of dense local structures.

213 The most intuitive way to select a node is to move the mouse cursor to the node and
214 then click. This requires mapping the screen cursor coordinates into the 3D SWC
215 space. Multiple selections should also be supported to specify a set of nodes as the

216 input of an operation. After selection, the user can trigger an operation with some
 217 input. So the operation becomes

$$f(S_1|\Theta) = S_2$$

218 where Θ is the set of parameters supplied from user input. For example,
 219 $f(\{\mathbf{n}\}|(x, y, z)) = \{\mathbf{n}, F_p((x, y, z, r(\mathbf{n})), \mathbf{n}_0, \mathbf{n}_0, \mathbf{n}_0)|\mathbf{n})\}$ defines an operation of
 220 extending a branch from \mathbf{n} to a node at (x, y, z) .

221

222 **2.1.4 Create SWC Nodes from Image Signal**

223 For any standalone neuron-tracing software, it is essential to allow reconstructing
 224 neuron structure from raw image signals. In the SWC framework, this function can
 225 be formulated as

$$g(S_1|\Theta, I) = S_2$$

226 where I is the image signal. Note that this actually defines a superfamily of SWC
 227 operations. The function is the same as an SWC operation if it is independent of I . An
 228 example of an image-dependent operation is shortest path creation, such as the one
 229 used by Simple Neurite Tracer (Longair et al., 2011), where $S_1 = \{\mathbf{n}_i, \mathbf{n}_j\}$ defines the
 230 source and target node and $S_2 = \{\mathbf{n}_i, \mathbf{n}'_1, \dots, \mathbf{n}'_k, \mathbf{n}_j\}$ forms the resampled shortest
 231 geodesic path from \mathbf{n}_i to \mathbf{n}_j . The radii of $\mathbf{n}'_1, \dots, \mathbf{n}'_k$, which are denoted as
 232 $r(\mathbf{n}'_1), \dots, r(\mathbf{n}'_k)$ in the node definition, can be estimated automatically or linearly
 233 interpolated, depending on how the operation is defined.

234

235 **2.2. Software Implementation**

236 **2.2.1 Architecture**

237 Based on the SWC framework, we have built neuTube 1.0 as a GUI application upon
238 four core modules: 2D visualization, 3D visualization, image analysis and neuron
239 structure operation (Figure 2).

240 **2.2.2 2D Visualization**

241 The 2D visualization module provides functions of displaying a 3D image and
242 neuron structures slice by slice, as well as functions allowing the user to interact
243 with the 2D display. This module facilitates close examination and precise editing.
244 For example, driven by this module, the user can zoom into a region of interest to
245 view details, locate tracing point precisely, or apply fine-tuning on a neuron
246 structure. As the purpose of 2D visualization is to show the matching quality
247 between the reconstruction and the data rather than a realistic neuron structure, we
248 only used two geometrical primitives, lines and circles, to represent the morphology
249 of a neuron (Figure 3B). The 2D visualization is useful for showing the exact planar
250 position of a node, yet not suitable for showing the position perpendicular to the
251 plane. We used two strategies to address the issue. First, each node of the neuron is
252 displayed as a circle when the plane cuts through the node. The circle is as large as
253 the corresponding cross section of the node, informing the user by its size how far
254 the node is from the plane. Second, we used colors to distinguish whether a node is
255 centered on the current plane (on-plane) or not (off-plane): the node is shown with
256 a fully saturated and opaque color when it is on-plane; otherwise the node color is
257 semi-transparent and less saturated (Figure 3B). The coloring options were tuned
258 manually according to the user feedback and then used as immutable parameters of

259 the software. To allow the user view the global structure of a neuron under
260 reconstruction, we also project the whole skeleton onto the slice view, but with a
261 thin and semi-transparent mode to minimize its interference with in-focus
262 structures.

263 **2.2.3 3D Visualization**

264 The 3D visualization module is designed to provide real-time rendering of 3D
265 images and neuron structures. The user can perform tracing (Figure 3D) and editing
266 (Figure 3F) in the 3D visualization window directly, in which any change in the
267 neuron structure will be reflected in the 2D visualization window simultaneously,
268 and vice versa.

269 This module supports both realistic neuron rendering and structural rendering by
270 decomposing a neuron structure into three geometric primitives, including sphere,
271 line and conical frustum. The user can choose to view a neuron as connected
272 spheres (Figure 3E), tubes (Figure 3G) or lines (Figure 3H) for checking different
273 morphological properties of the neuron. Besides the different view styles, the
274 module also provides multiple color modes for inspecting topological properties of a
275 neuron or dissecting multiple neurons.

276 **2.2.4 Image Analysis**

277 This module offers automatic tracing of a neuron or a neuron branch to allow the
278 user to obtain neuron structures with minimal interaction. For example, to select a
279 branch, the user only needs to specify a point on the branch with one click. The
280 algorithm and design were described in Zhao et al., (2011) and Kim et al., (2012). In
281 this paper one major improvement over the previously reported version (Kim et al.,

282 2012) is the replacement of the cylindrical model by the tree model defined in the
283 SWC framework. In addition, we have implemented a point-to-point tracing function
284 based on the shortest path method used previously in automated reconstruction
285 (Zhao et al., 2011). This function is similar to semi-automated tracing in the Simple
286 Neurite Tracer and Vaa3d, but we have made it available in both 2D and 3D views by
287 following the SWC framework.

288 **2.2.5 Neuron Structure Manipulation**

289 The module of neuron structure manipulation provides functions for the arbitrary
290 editing of neuron nodes (Figure 3C and Figure 3F). The user can change the
291 geometry and topology of a neuron structure with intuitive mouse clicks or
292 keyboard shortcuts. This module supports operations described in the SWC
293 framework, and separates them into different levels.

294 We have also built high-level operations from elementary ones to reduce the labor
295 required for structural operations. These operations are following listed.

296 **2.2.5.1 Interpolate**

297 In many cases, a neuron branch or a segment thereof is smooth enough to be
298 represented by piecewise linear structures. Interpolation takes advantage of this
299 property and allows the user to quickly correct geometrical attributes of multiple
300 nodes (Figure 4B) by specifying the nodes that need interpolation (Figure 4A).

301 **2.2.5.2 Set branch point**

302 It often happens that a branch point is missed when the end of a segment is close to
303 the interior of another segment. A completely manual editing operation would
304 consist of selecting two nodes and joining them together. The operation of setting

305 branch point simplifies this work by connecting the selected node (Figure 4C) to the
306 latest node in isolated branches when the connection creates a branch point (Figure
307 4D).

308 **2.2.5.3 Reset branch point**

309 This operation provides another way to correct a branch point. In this operation, the
310 user selects a node (Figure 4E) and the program will try to move the neighboring
311 branching structure to the selected node (Figure 4F). The program automatically
312 determines which branch to move based on their angles.

313 **2.2.5.4 Connect multiple nodes**

314 Connecting two nodes is one of the most basic operations, yet one that requires
315 multiple steps, including selecting the nodes and triggering the connection
316 command. When there are more and more nodes to connect, the number of human
317 interactions increases proportionally. Therefore, neuTube 1.0 provides an operation
318 for automatically connecting multiple nodes (Figure 4G) by their edges in the
319 minimal spanning tree of their pairwise distance graph (Figure 4H).

320 **2.2.5.5 Remove turn**

321 A turn is defined as three sequentially connected nodes that form an acute angle.
322 The node in the middle is the turning point and the other two nodes are the flank
323 nodes. The operation of removing a turn is to set the turning point (Figure 4I) as the
324 interpolation of the flank nodes (Figure 4J). When the turning point is a branch
325 point, the flank nodes are its two neighbors that form the sharpest turn.

326 **2.2.5.6 Resolve crossover**

327 Crossover is a common tracing error in tracing when two branches are close at a
328 certain point (Figure 4K). Correcting a crossover requires several operations of

329 connecting and breaking nodes. Therefore, we added an operation of automatic
330 inference of crossover (Figure 4L) to make the editing easier.

331 **2.2.6 Implementation**

332 The software is written in the C and C++ programming languages with several third-
333 party libraries. The main third-party library is the Qt library (<http://qt-project.org>),
334 which provides a cross-platform framework for GUI development. The 3D
335 visualization module is built upon OpenGL 2.0 (<http://www.opengl.org>) and its
336 shading language, GLSL (<http://www.opengl.org/documentation/glsl>). We
337 developed a fast engine for rendering neuron structures by writing highly efficient
338 shaders for two geometric primitives, sphere and conical frustum. The vertex
339 shader finds bounding boxes of the geometric primitives on the screen, and then the
340 fragment shader calculates ray-quadratic intersections for each pixel inside the
341 rasterized bounding box. All of our geometric primitives have adjustable opacity
342 options and can be visualized in the order needed to generate a reasonable semi-
343 transparent scene. For realistic rendering of complicated semi-transparent scenes,
344 we have also implemented Dual Depth Peeling and Weighted Average Blending
345 (Bavoil and Myers, 2008), which are two commonly used order-independent
346 transparency methods. Since the two methods do not require special hardware
347 features of high-end graphical cards, they provide neuTube 1.0 the ability of
348 rendering complicated scenes realistically without comprising the software
349 portability. The user can switch from one method to the other in runtime to
350 determine which one is better for the current scene.

351 To show an image signal in 3D, a volume, which contains the original image of the
352 neurons to reconstruct, is uploaded to GPU as 3D texture and is rendered by a
353 volume shader. The volume shader provides several volume composite methods,
354 including Direct Volume Rendering (DVR), Maximum Intensity Projection (MIP) and
355 its opaque variant, Local Maximum Intensity Projection (LMIP) (Sato et al., 1998).
356 Each method has its own advantages. For example, MIP opaque allows the user to
357 see weak signals that are typical of thin neural branches, LMIP is an extended
358 version of MIP that can clearly depict spatial interrelations of neural branches, and
359 DVR illustrates bright structures with low noise (Fishman et al., 2006). Users can
360 also trace interactively in a 3D view by providing a seed point for tracing with a
361 single mouse click, which represents a ray passing through the 3D volume. The seed
362 point used for tracing is determined as the first location with maximum intensity
363 along the ray.

364 **3. Results**

365 We compared our neuTube 1.0 to other neuron reconstruction softwares, namely,
366 Neuromantic and Neurostudio. These two softwares were chosen because their
367 designs are close to the SWC framework, although they lack several important
368 features available in the framework (Table 1). Four 3D images from the DIADEM
369 datasets (Brown et al., 2011) were traced using all three softwares by four users
370 given the same time constraint. Similar to the situation of real applications, the user
371 can decide to stop tracing whenever he/she could not identify or fix an error. This
372 reflects how well the software visualizes the reconstruction along with the data and

373 the flexibility of the editing functions. The accuracy of tracing was measured by how
374 well the critical points, including branching points and termini, were reconstructed
375 compared to ground truth reconstructions. We extracted branching and terminal
376 points as two point sets from each tracing result and matched them to the ground
377 truth by solving the Linear Assignment Problem (LAP) using the Jonker-Volgenant
378 Algorithm (Jonker and Volgenant, 1987). Assuming there are a total of N points with
379 M of them matched to the ground truth, the reconstruction error is calculated as:

$$\text{Error} = \frac{T_d(F_p + F_n) + \sum_{m=1}^M d_m}{N}$$

380 where F_p and F_n are the number of false positives and the number of false negatives
381 respectively, T_d is the maximal distance allowed between two matched points
382 (Figure 5A), and d_m is distance between the m th matched pair of points. In this
383 calculation, the term $T_d(F_p + F_n)$ is the cost of missing critical points and $\sum_{m=1}^M d_m$ is
384 the cost of position offset.

385 Our error metric is designed on the basis of the DIADEM metric (Gillette et al., 2011),
386 but with two major modifications for better evaluation of interactive neuron
387 reconstruction. One modification is that our metric matches critical points globally,
388 while the DIADEM metric matches critical points in a certain order, which starts
389 from the root position and may give an upstream node more importance. For user
390 editing, missing an upstream node and missing a downstream one usually mean the
391 same type of error. Our matching method is order-independent and treats these
392 nodes equally. The other different feature of our metric is the combination of
393 topological errors and position errors, with the introduction of the matching

394 threshold (T_d), as the weight of mismatches. The threshold T_d is similar to the
 395 threshold region of the DIADEM metric, but we do not assign it a fixed value, which
 396 is often subjective or application dependent. Instead, we define the error metric as a
 397 function of T_d .

398 By comparing scores across a wide range of threshold values, we showed that
 399 neuTube 1.0 achieved consistently better reconstruction accuracy than
 400 Neuromantic and Neurostudio (Figure 5B). The advantage of neuTube 1.0 is more
 401 significant when the threshold is larger, indicating that neuTube 1.0 helps the user
 402 obtain more accurate neuron structures by identifying more critical points than the
 403 other two software tools.

404

405

Feature comparison table

Software	Undo/Redo	2D Editing	3D Editing	3D Image Interaction	2D Neuron Visualization	3D Visualization
neuTube 1.0	Unlimited	Yes	Yes	Yes	Slice-by-Slice	Volume & Neuron Structure
Neuromantic	1 step	Yes	Limited ²	No	Slice-by-Slice	Neuron Structure
Neurostudio	1 step	Limited ¹	Limited ²	No	Projection	Volume & Neuron Structure

406

407

408

¹ Cannot change node size

² No topological operation

409 **4. Application Example**

410 We have used neuTube 1.0 to map the fine-scale synaptic connectivity between
 411 hippocampal regions (CA3-CA1) of the mouse brain (Druckmann et al., 2014). To
 412 analyze the spatial synaptic connectivity pattern, mammalian GFP reconstitution
 413 across synaptic partners (mGRASP) (Kim et al., 2012) was used to label the
 414 synapses, and red fluorescence protein (i.e. dTomato) was used to label the post-

415 synaptic dendrites (Figure 6A). neuTube 1.0 was used to reconstruct 3D structures
416 of post-synaptic neurons (Figure 6B). In our application, we detected the mGRASP-
417 labeled synapses using our mGRASP detection package (Feng et al., 2012) (Figure
418 6C), and then assigned each synapse to a reconstructed neuron by calculating its
419 intensity-weighted distances to all nearby neurons (Figure 6D). To make the
420 mapping more accurate in the step of synapse assignment, we need to reconstruct
421 not only the selected neurons but also the remaining dendrite branches or
422 background neurons (Figure 6B) because the distance to the nearest selected
423 neuronal branch alone can mis-assign synapse puncta (Feng et al., 2014). A practical
424 solution to this is to reconstruct all dendrite branches from the 3D image first and
425 then edit the target neurons, which must be reconstructed correctly. neuTube
426 turned out to be the right tool for this problem because the SWC framework
427 specifies that the software can start the reconstruction from any SWC file. With the
428 help of neuTube 1.0, we have built a fine-scale mapping of the hippocampal CA3-
429 CA1 circuit and, with further statistical analysis, revealed spatially structure and
430 clustered synaptic connectivity patterns between CA3 and CA1 (Druckmann et al.,
431 2014).

432 **5. Discussion**

433 We designed the SWC framework and implemented it in neuTube 1.0
434 (www.neutracing.com) to improve the efficiency of reconstructing neuron
435 structures accurately. Guided by the framework, the software combines 2D/3D
436 visualization, semi-automated tracing algorithms and flexible editing options to

437 simplify the task of neuron reconstruction. The SWC framework is not designed to
438 solve the problem of high-throughput neuron tracing, which is different and more
439 challenging. As revealed by the recent DIADEM competition (Liu, 2011), a reliable
440 and generally applicable high-throughput neuron-tracing tool may not be available
441 in the near future. While waiting for the ideal solution, neuroscientists will benefit
442 from better neuron reconstruction tools. Therefore, the goal of the SWC framework
443 is to provide a general architecture, which can adopt state-of-the-art image analysis
444 methods and modern software techniques, for building better interactive neuron
445 reconstruction tools.

446 Our framework has one limitation, which is that it can only produce neuron
447 structures defined in the SWC format. However, this is usually not a significant
448 concern because the SWC model suffices for most purposes, such as comparing
449 neuron shapes, performing Sholl analysis, uploading neuron structures to
450 NeuroMorpho.org (Ascoli et al., 2007), and simulating neuron activities. Many
451 researchers prefer the SWC format rather than more complicated models because it
452 helps to avoid overfitting to imaging artifacts: the resolution of optical microscopy is
453 usually not high enough to reveal fine details. Even when a structure more complex
454 than the SWC model is needed, reconstructing the neurons in the SWC model is still
455 useful as an initial input for later shape refinement (Evers et al., 2005).

456 Our experiment showed that the results from neuTube 1.0 were generally better
457 than those from Neurostudio (Myatt et al., 2012) and Neuromantic (Wearne et al.,
458 2005), but it is still worth noting the strengths of these softwares. Neuromantic
459 allows multi-tile tracing to reconstruct neurons from more than one field of view.

460 This is particularly useful for reconstructing a large neuron that requires horizontal
461 stage movement to cover all branches. Neurostudio offers only limited free editing
462 functions, but its ability to trace multiple branches from one seed point is a very
463 useful feature to reduce labor, and its intrinsic radius estimation based on rayburst
464 sampling (Rodriguez et al., 2006) can be implemented in any other software to
465 refine the neuron structure.

466 As the functions of multi-branch tracing and rayburst radius estimation naturally fit
467 in the SWC framework, we plan to include them in the future upgrade of neuTube
468 1.0. Additionally, there are ongoing efforts to extend the software to broader
469 applications, including tracing neurons in bright-field images and analyzing neuron
470 morphologies, such as identifying neuron types from electron microscope
471 reconstructions (Zhao and Plaza, 2014).

472 Because a user can import results from other software into neuTube 1.0 to do
473 further editing, neuTube 1.0 is also a complementary tool to other automated or
474 interactive neuron tracing tools. For instance, the Vaa3d software has added
475 neuTube 1.0 as a plug-in in recent releases (vaa3d.org). On the other hand, other
476 developers can improve their own software by adopting the SWC framework. To
477 facilitate any such adoption, we have made the source code of neuTube 1.0 available
478 at <https://github.com/janelia-flyem/NeuTu>.

479 **References**

- 480 Ascoli GA, Donohue DE, Halavi M (2007) NeuroMorpho.Org: a central resource for
481 neuronal morphologies. *J Neurosci* 27:9247–9251.
- 482 Bavoil L, Myers K (2008) Order independent transparency with dual depth peeling.
483 NVIDIA OpenGL SDK:1–12.

- 484 Brown KM, Barrionuevo G, Canty AJ, De Paola V, Hirsch JA, Jefferis GSXE, Lu J, Snippe
485 M, Sugihara I, Ascoli GA (2011) The DIADEM Data Sets: Representative Light
486 Microscopy Images of Neuronal Morphology to Advance Automation of Digital
487 Reconstructions. *Neuroinformatics* 9:143–157.
- 488 Cannon RC, Turner DA, Pyapali GK, Wheal HV (1998) An on-line archive of
489 reconstructed hippocampal neurons. *Journal of Neuroscience Methods* 84:49–
490 54.
- 491 Druckmann S, Feng L, Lee B, Yook C, Zhao T, Magee JC, Kim J (2014) Structured
492 Synaptic Connectivity between Hippocampal Regions. *Neuron* 81:629–640.
- 493 Evers JF, Schmitt S, Sibila M, Duch C (2005) Progress in functional neuroanatomy:
494 precise automatic geometric reconstruction of neuronal morphology from
495 confocal image stacks. *J Neurophysiol* 93:2331–2342.
- 496 Feng L, Kwon O, Lee B, Oh WC, Kim J (2014) Using mammalian GFP reconstitution
497 across synaptic partners (mGRASP) to map synaptic connectivity in the mouse
498 brain. *Nature Protocols* 9:2425–2437.
- 499 Feng L, Zhao T, Kim J (2012) Improved synapse detection for mGRASP-assisted
500 brain connectivity mapping. *Bioinformatics* 28:i25–i31.
- 501 Fishman EK, Ney DR, Heath DG, Corl FM, Horton KM, Johnson PT (2006) Volume
502 Rendering versus Maximum Intensity Projection in CT Angiography: What
503 Works Best, When, and Why1. *RadioGraphics* 26:905–922.
- 504 Gillette TA, Brown KM, Ascoli GA (2011) The DIADEM Metric: Comparing Multiple
505 Reconstructions of the Same Neuron. *Neuroinformatics* 9:233–245.
- 506 Jonker R, Volgenant A (1987) A shortest augmenting path algorithm for dense and
507 sparse linear assignment problems. *Computing* 38:325–340.
- 508 Kim J, Zhao T, Petralia RS, Yu Y, Peng H, Myers E, Magee JC (2012) mGRASP enables
509 mapping mammalian synaptic connectivity with light microscopy. *Nat Methods*
510 9:96–102.
- 511 Liu Y (2011) The DIADEM and Beyond. *Neuroinformatics* 9:99–102.
- 512 Long F, Zhou J, Peng H (2012) Visualization and Analysis of 3D Microscopic Images
513 Lewitter F, ed. *PLoS Comput Biol* 8:e1002519.
- 514 Longair MH, Baker DA, Armstrong JD (2011) Simple Neurite Tracer: open source
515 software for reconstruction, visualization and analysis of neuronal processes.
516 *Bioinformatics* 27:2453–2454.
- 517 Luisi J, Narayanaswamy A, Galbreath Z, Roysam B (2011) The FARSIGHT trace

- 518 editor: an open source tool for 3-D inspection and efficient pattern analysis
519 aided editing of automated neuronal reconstructions. *Neuroinformatics* 9:305–
520 315.
- 521 Meijering E (2010) Neuron tracing in perspective. *Cytometry* 77A:693–704.
- 522 Myatt DR, Hadlington T, Ascoli GA, Nasuto SJ (2012) Neuromantic - from semi-
523 manual to semi-automatic reconstruction of neuron morphology. *Front*
524 *Neuroinform* 6:4.
- 525 Peng H, Long F, Zhao T, Myers E (2011) Proof-editing is the bottleneck of 3D neuron
526 reconstruction: the problem and solutions. *Neuroinformatics* 9:103–105.
- 527 Peng H, Ruan Z, Long F, Simpson JH, Myers EW (2010) V3D enables real-time 3D
528 visualization and quantitative analysis of large-scale biological image data sets.
529 *Nature Biotechnology* 28:348–353.
- 530 Rodriguez A, Ehlenberger DB, Hof PR, Wearne SL (2006) Rayburst sampling, an
531 algorithm for automated three-dimensional shape analysis from laser scanning
532 microscopy images. *Nature Protocols* 1:2152–2161.
- 533 Sato Y, Shiraga N, Nakajima S, Tamura S, Kikinis R (1998) Local Maximum Intensity
534 Projection (LMIP): A New Rendering Method for Vascular Visualization. *Journal*
535 *of Computer Assisted Tomography* 22:912–917.
- 536 Wearne SL, Rodriguez A, Ehlenberger DB, Rocher AB, Henderson SC, Hof PR (2005)
537 New techniques for imaging, digitization and analysis of three-dimensional
538 neural morphology on multiple scales. *Neuroscience* 136:661–680.
- 539 Zhao T, Plaza SM (2014) Automatic Neuron Type Identification by Neurite
540 Localization in the *Drosophila* Medulla. arXiv q-bio.NC:1409.1892.
- 541 Zhao T, Xie J, Amat F, Clack N, Ahammad P, Peng H, Long F, Myers E (2011)
542 Automated reconstruction of neuronal morphology based on local geometrical
543 and global structural models. *Neuroinformatics* 9:247–261.

544

545 **Legends**

546 **Tables**

547 Table 1: Feature comparison of neuTube 1.0 with Neuromantic and Neurostudio.
548

549 **Figures**

550 Figure 1 Workflow of reconstructing or editing a neuron structure in the SWC framework,
551 which defines GUI software that takes either a raw image or an SWC file as input and

552 generates an acceptable neuron structure through user interactions. The user can save the
553 neuron structure into standard SWC files during or after reconstruction.

554

555 Figure 2 neuTube 1.0 is a GUI application built upon four major modules, including 2D
556 visualization, 3D visualization, image analysis and neuron structure operation.

557

558 Figure 3 Tracing and editing interface of neuTube 1.0. (A) Interactive tracing in 2D view. (B)
559 2D view of SWC nodes. On-plane and off-plane nodes are distinguished by color saturation
560 and transparency. A node with a yellow bounding box indicates that it is selected. (C) The
561 context menu for editing in the 2D view, which can be triggered by a right mouse click. (D)
562 Interactive tracing in 3D view. (E) 3D visualization of the tracing results. Branch nodes and
563 terminal nodes are shown in green and yellow colors respectively. Selected nodes are
564 shown with their bounding boxes. (F) The context menu for editing in the 3D view. (G) A
565 neuron shown as connected tubes. (H) A neuron shown as lines.

566

567 Figure 4 Examples of high-level operations of neuTube 1.0. To illustrate the operation, we
568 visualize the nodes of a neuron in different colors according to the topology: blue for root nodes,
569 green for branch nodes, yellow for leaf nodes and red for other nodes. Selected nodes are
570 highlighted by a yellow bounding box. For the corresponding operation as named in each row,
571 the figure on the left (A), (C), (E), (G), (I) or (K) shows the selected nodes to operate and the one
572 on the right (B), (D), (F), (H), (J) or (L) shows the result of operation.

573

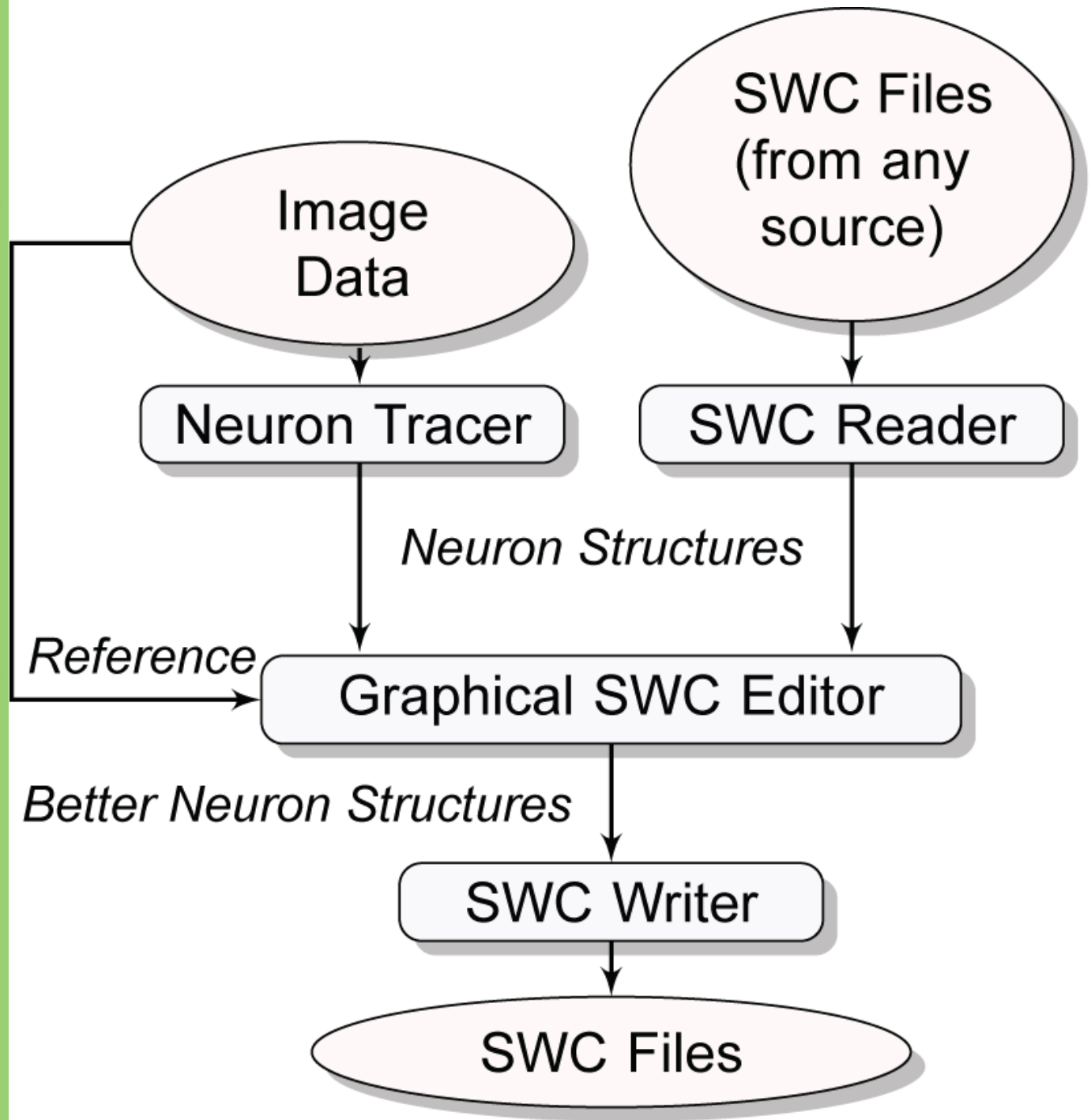
574 Figure 5 neuTube 1.0 helps produce significantly more accurate neuron structures than
575 Neuromantic and Neurostudio do. (A) Node_g is a critical point from ground truth neuron
576 and Node_t is a critical point from tracing result. These two points can be matched when
577 $T_d = T_{d2}$ because the distance between them is less than T_{d2} . They cannot be matched when
578 $T_d = T_{d1}$. (B) The solid curves show average errors measuring the discrepancy between the
579 critical point sets from user reconstruction and ground truth under different distance
580 thresholds. The surrounding envelopes are the 95% confidence intervals. The error curve of
581 neuTube 1.0 (green) is consistently lower than the other two, with p value < 0.01 (t-test)
582 when $T_d \geq 6$ (compared to Neurostudio) or $T_d \geq 5$ (compare to Neuromantic).

583

584 Figure 6 Mapping brain connectivity with neuTube 1.0. (A) The original 3D confocal image
585 contains post-synaptic neurons. (B) The target neuron (green) was traced semi-
586 automatically. The red branches belong to background neurons. (C) mGRASP-labeled
587 synapses (yellow) were detected automatically, with sizes enlarged for better visualization.
588 (D) The synapses were mapped to the target neuron (green) and background neurons (red).

589

590



User Interface

Application

Graphical Users Interface

Engine

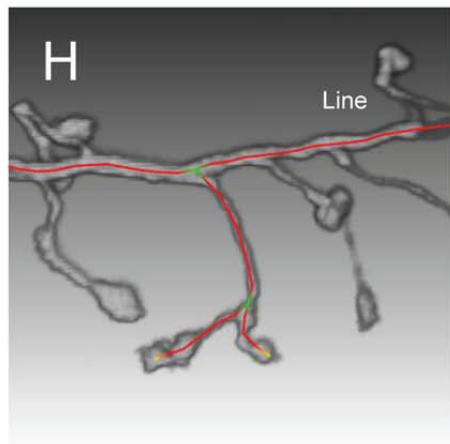
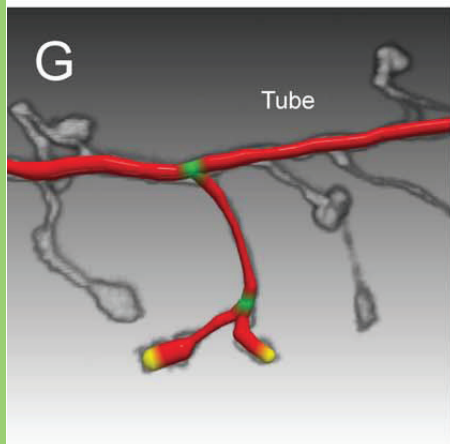
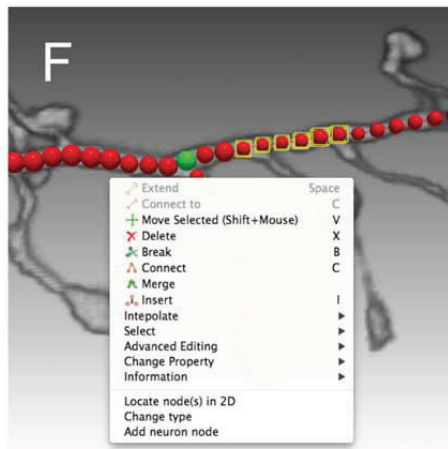
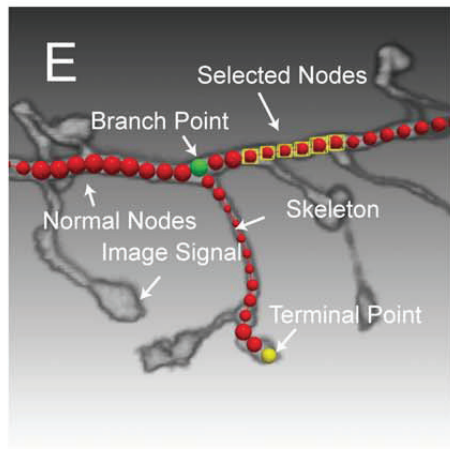
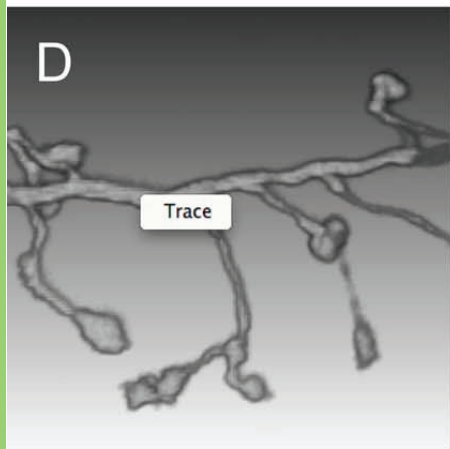
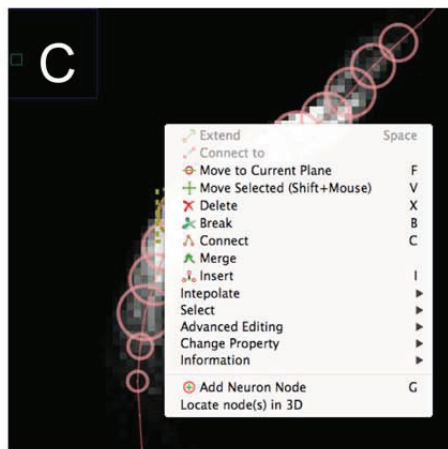
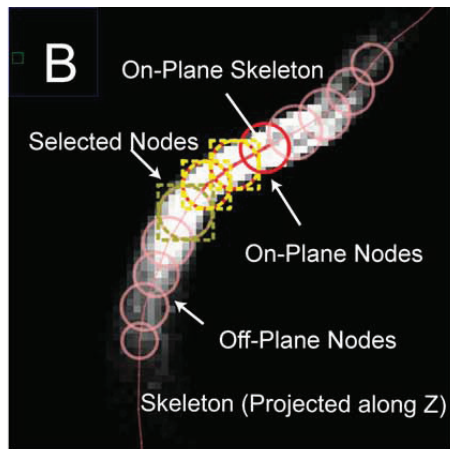
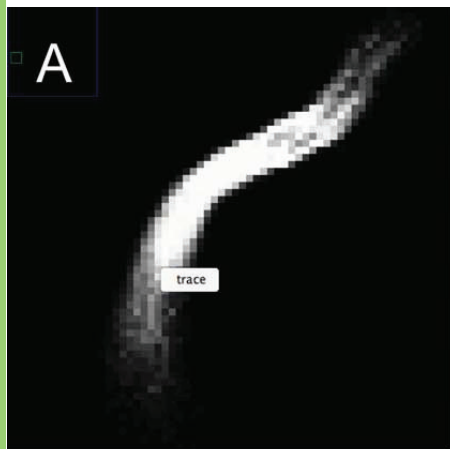
2D
Visualization

3D
Visualization

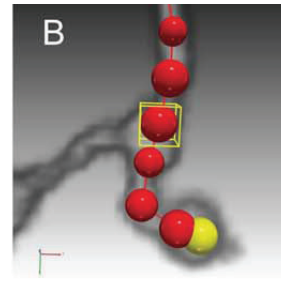
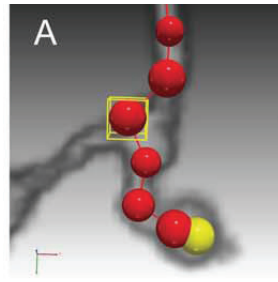
Image
Analysis

Neuron
Structure
Operation

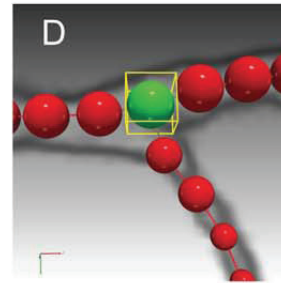
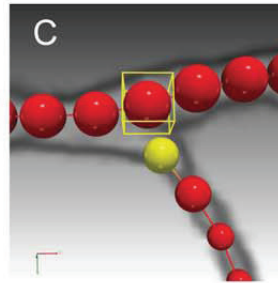
C/C++ Libraries (Qt, libXml, libGlew, ...)



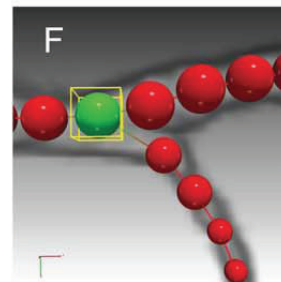
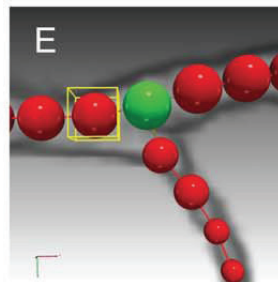
Interpolate



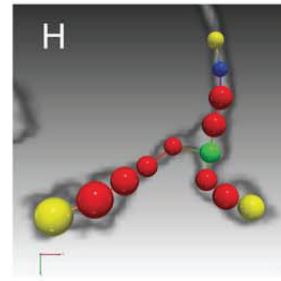
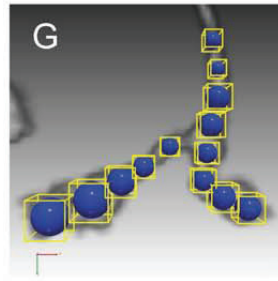
Set Branch Point



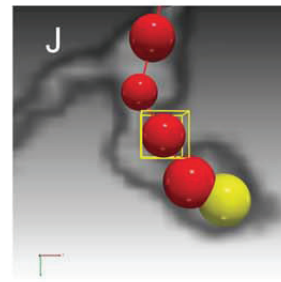
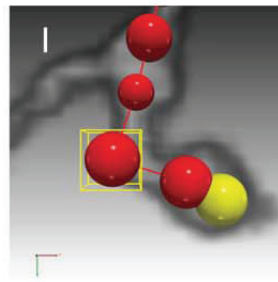
Reset Branch Point



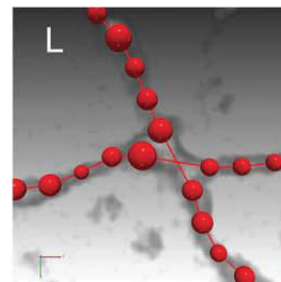
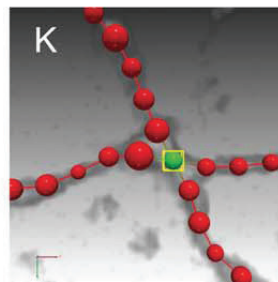
Connect Multiple Nodes

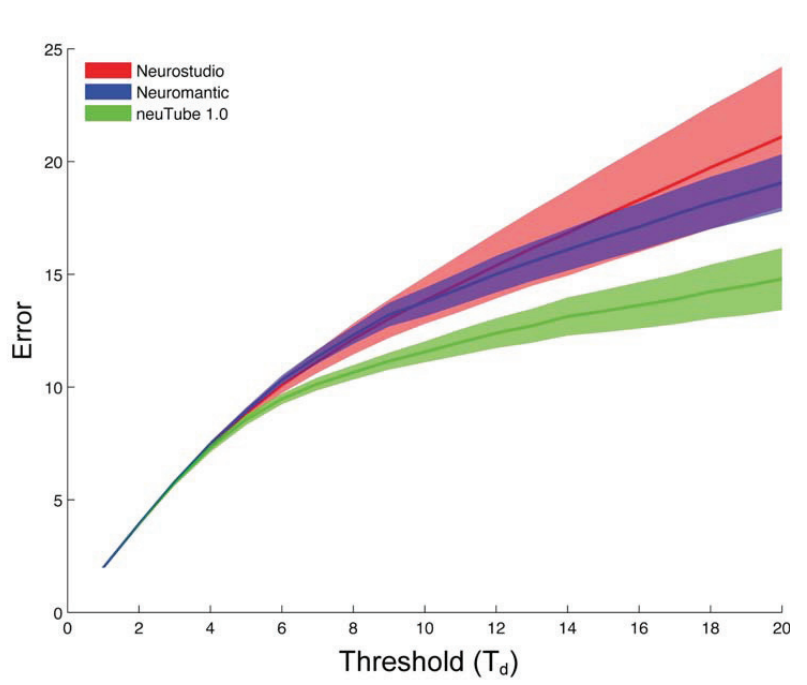
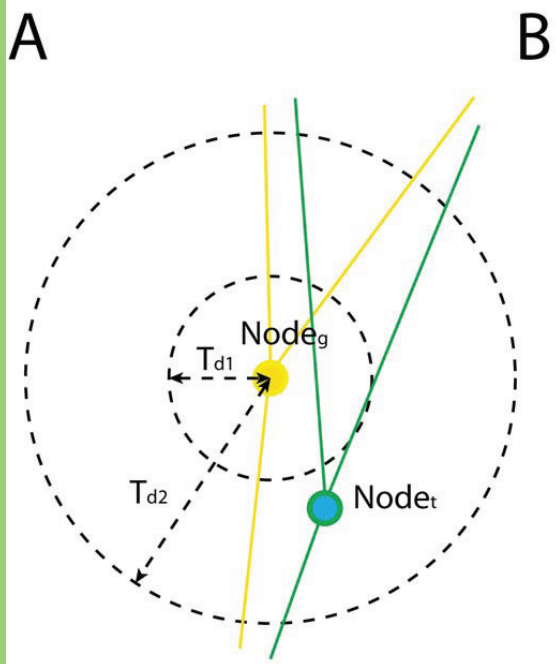


Remove Turn

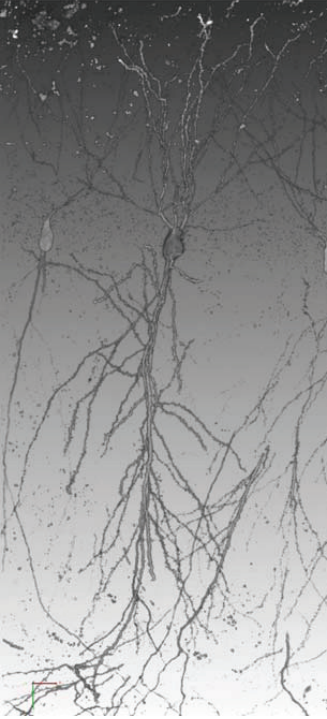


Resolve Crossover

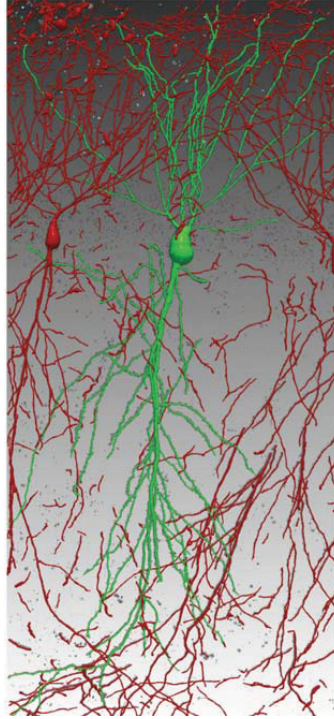




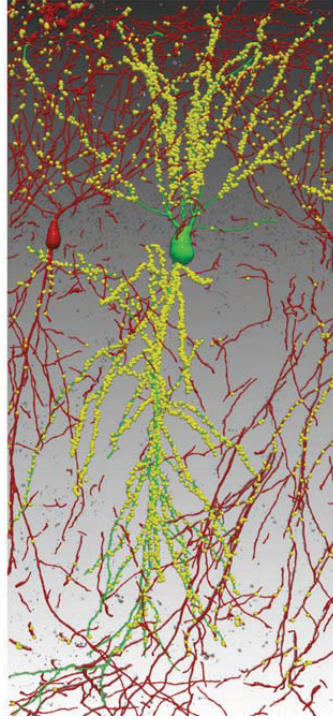
A
Image



B
Reconstruction



C
Detection



D
Mapping

